

# KRT23 as a Potential Target for Metabolic Dysfunction-Associated Fatty Liver Disease (MAFLD): Evidence From Bioinformatics Analysis, Human Gene Polymorphism and Animal Experiments

Yangmin Hao<sup>1,2,\*</sup>, Tao Zhang<sup>3,\*</sup>, Shaliyan Tuerxunmaiti<sup>1,2,\*</sup>, Ye Tian<sup>1,4,\*</sup>, Xinyu Wang<sup>1,2</sup>, Zhiming Li<sup>5</sup>, Liang Zhao<sup>6</sup>, Lei Bai<sup>7</sup>, Qu Chen<sup>8</sup>, Cheng Li<sup>9</sup>, Ayiguzhali Abulitipu<sup>1,2,10</sup>, Rui Wang<sup>1,11</sup>, Sheng Jiang<sup>1,2</sup>, Guoli Du<sup>1,2,11</sup>

<sup>1</sup>State Key Laboratory of Pathogenesis, Prevention, and Treatment of High Incidence Diseases in Central Asia, Urumqi, Xinjiang, People's Republic of China; <sup>2</sup>Department of Endocrinology, First Affiliated Hospital of Xinjiang Medical University, Urumqi, Xinjiang, People's Republic of China; <sup>3</sup>Department of Human Resources, First Affiliated Hospital of Xinjiang Medical University, Urumqi, Xinjiang, People's Republic of China; <sup>4</sup>Department of Vascular Thyroid Surgery, Digestive Vascular Center, First Affiliated Hospital of Xinjiang Medical University, Urumqi, Xinjiang, People's Republic of China; <sup>5</sup>Department of Ultrasound, First Affiliated Hospital of Xinjiang Medical University, Urumqi, Xinjiang, People's Republic of China; <sup>6</sup>Department of General Medicine (General Surgery), First Affiliated Hospital of Xinjiang Medical University, Urumqi, Xinjiang, People's Republic of China; <sup>7</sup>Department of Hepatobiliary Surgery, First Affiliated Hospital of Xinjiang Medical University, Urumqi, Xinjiang, People's Republic of China; <sup>8</sup>Department of Information Management Section, First Affiliated Hospital of Xinjiang Medical University, Urumqi, Xinjiang, People's Republic of China; <sup>9</sup>Department of Data Statistics and Analysis Center of Operation Management, First Affiliated Hospital of Xinjiang Medical University, Urumqi, Xinjiang, People's Republic of China; <sup>10</sup>Department of General Medicine, Xinjiang Production and Construction Corps Hospital (Second Affiliated Hospital of Shihezi University), Urumqi, Xinjiang, People's Republic of China; <sup>11</sup>Department of Endocrinology, Bayingolin Mongolian Autonomous Prefecture People's Hospital, Kuerle, Xinjiang, People's Republic of China

\*These authors contributed equally to this work

Correspondence: Sheng Jiang; Guoli Du, Email xjjsh@126.com; genemagic@126.com

**Background:** Metabolic dysfunction-associated fatty liver disease (MAFLD) is highly prevalent in Xinjiang, with genetic factors influencing its pathogenesis. Keratin 23 (KRT23), a liver-enriched protein linked to metabolic regulation, remains understudied in MAFLD genetics.

**Objective:** To investigate associations between KRT23 gene polymorphisms, expression, and MAFLD in Xinjiang.

**Methods:** This study enrolled 1,795 MAFLD patients diagnosed via ultrasonography and metabolic criteria. KRT23 polymorphisms (rs72826004, rs2269859) were analyzed. GEO database screening identified MAFLD-related genes. KRT23 expression was assessed in human serum/liver tissues (ELISA, Western blot, qRT-PCR, IHC) and murine models (high-fat diet-induced MAFLD and db/db mice).

**Results:** Enrichment analysis identified 10 key MAFLD-associated genes, including KRT23. The rs72826004 TT genotype increased MAFLD risk (OR: 2.156, P=0.007), while rs2269859 TT conferred protection (OR: 0.306, P=0.002). MAFLD patients exhibited elevated KRT23 protein/mRNA levels in serum and liver versus controls. Murine models confirmed higher KRT23 expression in MAFLD and db/db mice compared to wild-type.

**Conclusion:** KRT23 gene polymorphism was associated with the occurrence of MAFLD. The rs72826004 loci TT genotype may be a risk factor for MAFLD, whereas the rs2269859 loci TT genotype may be a protective factor against MAFLD. Higher KRT23 expression (protein and mRNA) is related to MAFLD. KRT23 is a potential target for the treatment of MAFLD.

**Keywords:** metabolic dysfunction-associated fatty liver disease, MAFLD, bioinformatics, gene polymorphism, keratin 23, KRT23, clinical data and animal experiments

## Introduction

Metabolic dysfunction-associated fatty liver disease (MAFLD) is a condition characterized by the accumulation of excess fat in the livers of people who consume little to no alcohol.<sup>1–3</sup> MAFLD has become increasingly common, affecting approximately 25% of the population, and is related to several metabolic risk factors, such as hypertension, diabetes, insulin resistance, obesity and dyslipidemia.<sup>4–8</sup> MAFLD is complex and cannot be fully explained through one pathogenesis.<sup>9</sup>

In addition to the proven mechanisms, other potential new targets affecting the pathogenesis of MAFLD have not yet been systematically identified.<sup>10</sup> Exploring public databases and obtaining valid information for MAFLD diagnosis and treatment is valuable to increase the prediction accuracy, early detection rate and cure rate.<sup>11</sup>

Expressed in a tissue-specific manner, keratins (KRTs) are accepted as structural proteins that have intermediate filaments of epithelial cells.<sup>12</sup> The keratin family consists of 54 proteins from two families (type I, acidic, and type II, neutral or alkaline).<sup>13</sup>

Keratin interacts with other proteins or members of the KRT family through various epigenetic modifications, exerting significant effects on the stress response, progression of multiple cancers, and signaling pathways.<sup>14</sup>

As a member of the KRT type II family, the KRT23 gene is located on chromosome 17q21.2 and expresses a 1.65 kb mRNA with a molecular weight of 48 kDa.<sup>15</sup> KRT23 is considered as a stress-induced ductal response marker, and its levels are correlated with liver disease severity.<sup>12</sup> In chronic liver disease, K23 expression is increased in patients with more pronounced inflammation/fibrosis. Significant upregulation (>200 fold) was observed in patients with acute liver failure (ALF) and end-stage primary biliary cholangitis (PBC).<sup>12</sup> Starman et al found that KRT23 was overexpressed in steatohepatitis livers compared with normal livers, and patients with steatohepatitis presented an advance degree of fibrosis.<sup>16</sup> Odena et al reported that KRT23 overexpression in patients with alcoholic hepatitis (AH) was driven by LPS/TLR4, and KRT23 is one of the most upregulated genes in AH, a novel biomarker for ductal cells, and is associated with disease severity.<sup>17</sup>

In addition to the above, KRT23 also regulates lipid droplet dynamics through PPAR  $\alpha$  co activation.<sup>18</sup> Although previous studies have linked KRT23 overexpression to alcoholic hepatitis, our work reveals its MAFLD specific regulatory paradigm. However, whether KRT23 is associated with MAFLD remains to be explored.

In this study, we used bioinformatics analysis to explore differentially expressed genes (DEGs) in MAFLD. Functional enrichment revealed KRT23's co-expression network with PPAR $\alpha$  and CYP7A1, suggesting its involvement in lipid homeostasis.

We sequenced two single nucleotide polymorphisms (SNPs) of the KRT23 gene in all individuals, and the differences in the distribution frequencies of these SNPs were compared between patients with and without MAFLD.

We analyzed KRT23 expression in the serum and liver and its association with MAFLD. To confirm this result, MAFLD animals, including C57/6L mice fed a high-fat diet and db/db (hereditary diabetic leptin receptor mutant) mice, were used to test KRT23 expression.

## Methods

### Data Extraction

We obtained data from the Gene Expression Omnibus (GEO) (<https://www.ncbi.nlm.nih.gov/geo/>).<sup>19</sup> The Metabolic dysfunction-Associated Steatohepatitis (MASH) dataset GSE89632 (GPL14951 platform) included 24 non-NASH individuals and 19 patients with NASH (MASH is the updated name for NASH<sup>20</sup> MASH is a severe type of MAFLD, [Supplementary Table 1](#)).

### Identification of DEGs

The DEGs between patients and the control group were analyzed using R software<sup>19,21</sup> with adjusted  $P < 0.05$ ;  $\log_2FC > 1$  indicated upregulated DEGs, and  $\log_2FC < -1$  indicated downregulated DEGs.

### GO and KEGG Pathway Enrichment

DEGs were subjected to Kyoto Encyclopedia of Genes and Genomes (KEGG), domain and Gene Ontology (GO) annotation and functional enrichment analysis using the KEGG database (<http://www.kegg.jp/kegg/mapper.html/>), InterPro domain database (<http://www.ebi.ac.uk/interpro/>) and UniProt-GOA database (<http://www.ebi.ac.uk/GOA/>).

The functional enrichment analysis of the DEGs was performed using a two-tailed Fisher's exact test. Statistical significance was set at adjusted  $P < 0.05$ .

## PPI Network Construction and Hub Gene Extraction

All DEG database accessions or sequences were searched against the Search Tool for the Retrieval of Interacting Genes (STRING) database version 11.0. Protein-protein interactions (PPIs) between the proteins belonging to the searched dataset were selected, and external candidates were excluded. Confidence score was used to define interaction confidence. We retrieved all interactions that had a confidence score  $\geq 0.7$  (high confidence).

## Expression Quantitative Trait Loci (eQTL)

eQTLs are genomic loci that explain changes in gene expression levels, most of which are SNP loci. The positive or negative values of the slope columns in the eQTL data corresponding to the mutant loci indicate an increase or decrease in gene expression levels. Linear regression analysis was used to investigate the correlation between genotypes (the TT genotype of the KRT23 gene rs72826004 and rs2269859 loci) and gene expression (plasma protein) MAFLD patients. The specific R packages and parameter settings used in all bioinformatics analyses above are listed in [Supplementary Table 2](#).

## Study Population

As shown in [Figure 1](#), 1820 patients who were treated at the First Affiliated Hospital of Xinjiang Medical University between January 1, 2022 and October 31, 2024 were included in the study. Eleven patients who met the inclusion and

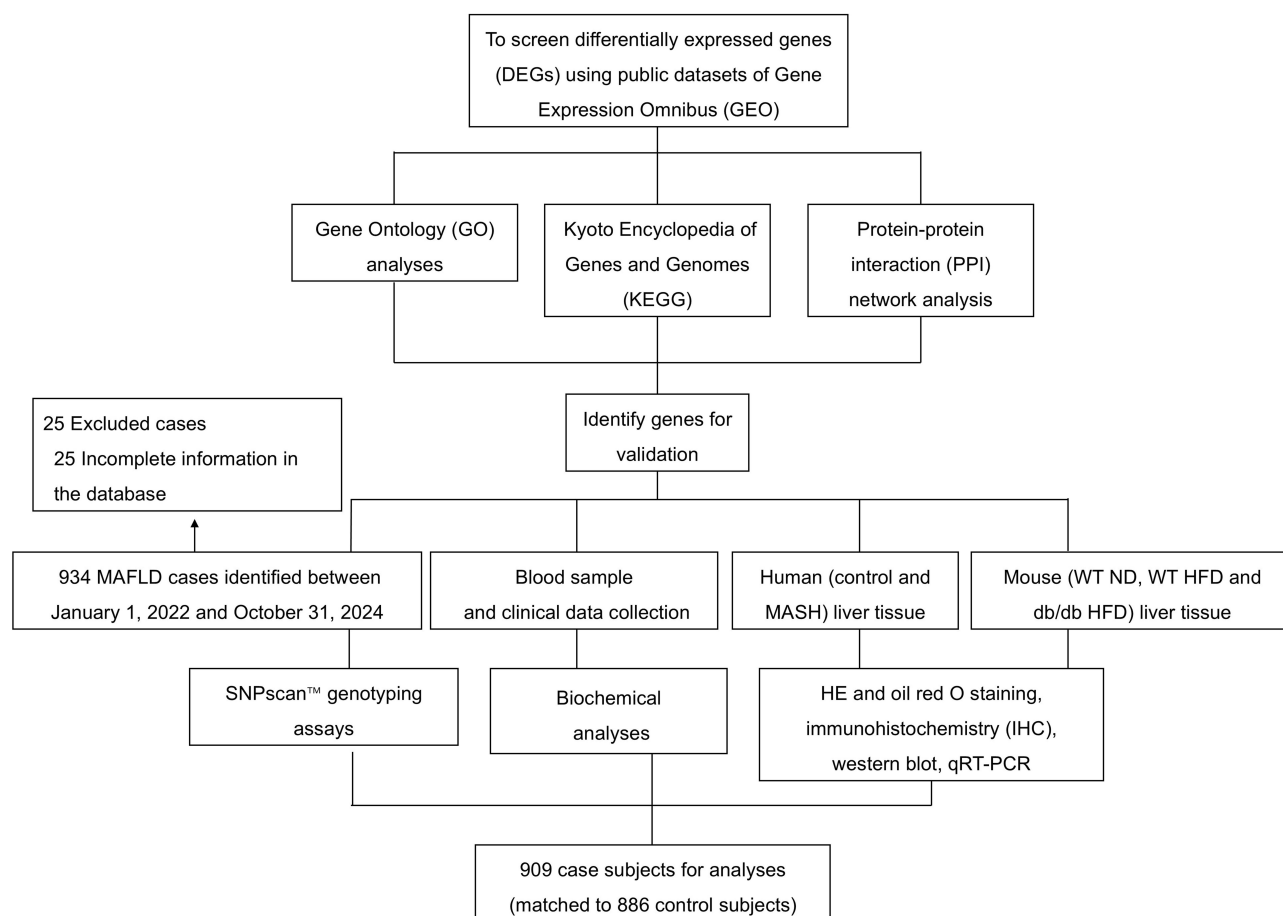


**Figure 1** Flow chart of the study.

**Abbreviations:** MAFLD, Metabolic dysfunction-associated fatty liver disease; MASH, Metabolic dysfunction associated steatohepatitis; WT ND, Wild type (C57BL/6) mice fed normal diet; WT HFD, Wild type mice fed high-fat diet; db/db mice, hereditary diabetic leptin receptor mutant mice; qRT-PCR, quantitative reverse transcription polymerase chain reaction.

exclusion criteria were randomly selected for liver tissue collection. The experiment was approved and conducted in accordance with the relevant guidelines established by the Ethics Committee of the First Affiliated Hospital of Xinjiang Medical University with the approval numbers IACUC-20230321-85, K202306-14, and 210104-05. All patients provided written consent for their samples to be collected.

### Inclusion Criteria

(a) Patients aged 18 years or older; (b) MAFLD was diagnosed when the frequency of steatosis hepatocytes exceeded 5%;<sup>22</sup> (c) rely on non-invasive screening ultrasound to diagnose MAFLD: Enhanced liver echo: liver parenchymal echo>renal cortex (“bright liver”); and (d) liver tissue with a MASH (Metabolic dysfunction-associated steatohepatitis) activity score (MAS) greater than 4 was diagnosed as MASH.

### Exclusion Criteria

(a) Patients with excessive alcohol consumption (>30 g/d for men and 20 g/d for women); (b) subjects with chronic liver disease from other etiologies (such as viral hepatitis or autoimmune hepatitis); (c) subjects who were diagnosed with liver cancers or other extrahepatic malignancies; and (d) subjects whose steatosis was < 5% on liver biopsy.<sup>23,24</sup>

### Diagnostic Criteria for MAFLD Patients

1. Evidence of metabolic abnormalities (at least 1 item): a) BMI  $\geq 25$  (Asia  $\geq 23$ ) or diabetes; b) Metabolic syndrome ( $\geq 2$  items): Abdominal obesity (male  $\geq 90$  cm/female  $\geq 80$  cm), hypertension ( $\geq 130/85$  mmHg), hyperglycemia ( $\geq 5.6$  mmol/L), hyper triglycerides ( $\geq 1.7$  mmol/L), low HDL (male<1.0/female<1.3).
2. Organizational characteristics: a)  $\geq 5\%$  hepatic steatosis; b) I (0–3 points); c) Fibrosis staging: 0 (none), 1 (sinus/portal), 2 (fibrous septum), 3 (bridging), 4 (cirrhosis).<sup>25</sup>

### General Data Collection

General data of non-MAFLD and MAFLD individuals, including sex, age, body mass index (BMI), smoking status, alcohol intake, history of hypertension, type 2 diabetes mellitus (T2DM), and family history of coronary artery disease (CAD), systolic blood pressure (SBP) and diastolic blood pressure (DBP) were collected according to the inclusion criteria. Laboratory tests for blood glucose, lipids, including cholesterol (TC), triglycerides (TG), high-density lipoprotein cholesterol (HDL-C) and low-density lipoprotein cholesterol (LDL-C), and imaging data, including ultrasound (US), computed tomography (CT), and magnetic resonance imaging (MRI), were also collected.

### Diagnosis of MAFLD, CAD and T2DM

MAFLD was diagnosed by experienced clinicians according to the following criteria: proposed criteria for a positive diagnosis of MAFLD are based on histological (biopsy), imaging or blood biomarker evidence of fat accumulation in the liver (hepatic steatosis) in addition to one of the following three criteria, namely, overweight/obesity, the presence of T2DM, or evidence of metabolic dysregulation.<sup>25</sup> Hepatic steatosis assessment includes clinical algorithms, imaging techniques (US, CT, and MRI), and liver biopsy.<sup>26</sup> T2DM was diagnosed on the basis of plasma glucose criteria, either the fasting plasma glucose (FBS) or 2 h plasma glucose during a 75 g oral glucose tolerance test, or hemoglobin A1c (HbA1c) criteria.<sup>27</sup> The typical symptom of CAD is exertional angina, with pressure pain in the precordial region during activity or emotional stress. The pain can radiate to the left shoulder or/and left upper arm for 5–10 min and can be relieved by rest or medications such as nitroglycerin. The diagnosis of CAD is based on symptoms, signs and ancillary tests such as electrocardiography (ECG) and coronary angiography (CAG). CAG is the gold standard for diagnosing CAD. The diagnosis of CAD should be at least one coronary arterial stenosis of 50% or its major branches in the CAG.<sup>28</sup>

### Genotyping Assay

Two SNPs (rs72826004 and rs2269859) of the KRT23 gene with minor allele frequencies (MAFs) greater than 5% were selected from the HapMap human SNP database ([www.hapmap.org](http://www.hapmap.org)) ( $R^2 \geq 0.8$  as a cutoff in linkage disequilibrium pattern analysis).<sup>29</sup> A total of 5 mL of fasting peripheral venous blood was drawn from the subjects into

ethylenediaminetetraacetic acid (EDTA)-containing blood collection tubes, and the plasma and blood cells were separated through centrifugation and stored in a  $-80^{\circ}\text{C}$  refrigerator until further use. Plasma was measured by biochemical indicators, and blood cells were subjected to genomic DNA extraction using a whole-blood genome extraction kit (Tiangen Biotech, China). Genomic DNA was isolated from whole blood. Genotyping for KRT23 rs72826004, rs2259859 was conducted using SNPscan technology, with technical assistance from Center for Genetic and Genomic Analysis, Genesky Biotechnologies Inc. (Shanghai, China, Primer sequence in [Supplementary Table 3](#)). For quality control and validation purposes, a random 5% of sample was repeated genotyping to check for consistency, and the results were 100% consistent.

## Hardy Weinberg Equilibrium (HWE) Test

After SNP typing, the genetic balance of genotype distribution in the control group was evaluated using the Hardy Weinberg equilibrium (HWE) test ([Supplementary Table 4](#)). The distribution of rs2269859 loci and rs72826004 loci conforms to HWE.

## Animals

Wild-type (WT) C57BL/6 mice were obtained from the Animal Center of Xinjiang Medical University. At the age of 8–9 weeks, the mice were fed either normal chow (growth and reproduction feed SPF grade (Co60 irradiation), MD17111, Medicience, Jiangsu, China) or a 60% fat/kcal diet (HFD, MD12033, Medicience, Jiangsu, China) for up to 16 weeks. Body weights were recorded weekly. The animals were housed in captivity in a specific pathogen-free environment on a 12-h light/dark cycle and were fed rodent chow and ad libitum water at the Xinjiang Medical University animal facility. All the mice received humane care according to the guidelines of the Medical Research Center, and all the experimental protocols were approved by the Ethics Committee of the First Affiliated Hospital of Xinjiang Medical University. All surgeries were performed under inhalation anesthesia with isoflurane, and every effort was made to minimize pain.

## Histological Analysis

Fresh liver tissue samples were fixed in 4% paraformaldehyde for 24 h, embedded in paraffin and sectioned into 5- $\mu\text{m}$  thick slices. For hematoxylin and eosin (H&E) staining, the sections were stained with hematoxylin and eosin solution (Solarbio, Cat# G1120, China). All the stained liver slides were observed using a light microscope, and the NAS was evaluated according to a previous report.<sup>30</sup>

Briefly, hepatic steatosis, lobular inflammation, and hepatic ballooning were investigated. Steatosis was scored on a scale of 0–3 according to the following criteria: 0 (<5%), 1 (5%–33%), 2 (33%–66%), or 3 (>66%). Lobular inflammation was scored on a scale of 0–3 according to the following criteria: 0 (no foci), 1 (<2 foci per 20 $\times$  optical field), 2 (2–4 foci per 20 $\times$  optical field), or 3 (>4 foci per 20 $\times$  optical field). Hepatocellular ballooning was scored on a scale of 0–2 according to the following criteria: 0 (none), 1 (mild, few), or 2 (moderate, many).

## Oil Red O Staining and Quantification

Liver sections were stained with Oil Red O solution (Solarbio, Cat# G1261, China) for 30 min, counterstained with hematoxylin to visualize lipid deposition. Randomly select 5 non-overlapping fields of view (20 $\times$  objective lens) for each liver slice, use ImageJ software to quantify the proportion of lipid droplet area, and take the average of three independent experiments for data. Quantitative analysis was performed via ImageJ v1.53 (NIH) with: 1. Spectral thresholding: 480–550 nm for Oil Red O signal isolation; 2. Morphometric calculation: (Positive pixel area / Total tissue area)  $\times$  100%.

## Immunohistochemistry and Quantification

For the IHC assays, the tissue sections were dewaxed, subjected to antigen retrieval, blocked with 10% goat serum, incubated with anti-KRT23 antibodies (Santa Cruz Biotechnology) at  $4^{\circ}\text{C}$  overnight, and then incubated with secondary antibodies for 30 min. Nuclei were stained with DAB, hematoxylin, and hydrochloric acid. Finally, the sections were scanned and observed under a microscope. The tissue sections were scanned by 3DHistech (Pannoramic MIDI,

Hungary). The details of the antibodies used are listed in [Supplementary Table 5](#). The relative quantification of targets in the IHC assays was dependent on the average optical density (AOD) evaluated by Image J software (NIH, USA).

## IHC Quantification

Each group consists of 3 biological replicates, with 5 random fields of view per sample. Quantify and calculate the AOD (IntDen/Area) for each field of view using ImageJ software, and take the average of  $\pm$  SEM within the group. Use analysis of variance or non-parametric tests to compare differences between groups. Integral density (IntDen)=total optical density of all pixels within the selected area; Area=pixel area of the selected region; AOD=IntDen/Area.

## Western Blotting

According to the manufacturer's instructions, proteins were extracted from fresh frozen tissues using RIPA lysis buffer and 1 mm PMSF (Solarbio, P8340, China). BCA assay kit was used to determine concentration (Solarbio, PC0020, China), and all surgeries were performed on ice. Each group of samples was loaded with 20  $\mu$ g of total protein. It was separated by 10% SDS polyacrylamide gel electrophoresis and transferred to polyvinylidene fluoride (PVDF) membrane. Seal the membrane with 5% skim milk (BioFroxx, 1172GR500) for 2 hours, incubate overnight with the first antibody at 4 °C ([Supplementary Table 5](#)), and then incubate with the second antibody. Protein levels were detected and evaluated by Bio Rad ChemiDoc MP chemiluminescence gel imaging system (California, USA). Normalize the relative expression level to the level of endogenous control (GAPDH) and use ImageJ software to quantify based on grayscale values (Relative expression level=target protein grayscale value/reference protein grayscale value, KRT23/GAPDH ratio).

## Nucleic Acid Isolation, Reverse Transcription PCR and Quantitative Real-Time PCR (qRT-PCR)

All the reagents used were treated with RNase removal reagent. Total RNA was isolated from tissues with TRIzol reagent (Thermo Fisher, USA). The concentration and quality of the RNA were assessed via a NanoDrop 2000 (Thermo Fisher). The RNA was stored at  $-80$  °C until use, and complementary DNA was synthesized with reverse transcription reagents (Takara#RR037A, Japan) according to the manufacturer's instructions. qRT-PCR was used to detect the relative transcription of target genes using ChamQ Universal SYBR qPCR Master Mix (Takara#RR820A, Japan). The samples were normalized to the expression of GAPDH using the  $2^{-\Delta\Delta CT}$  method.<sup>31</sup> The sequences of the primers are shown in [Supplementary Table 6](#).

## Enzyme-Linked Immunosorbent Assay (ELISA)

Serum samples were collected from patients, and mice were stored at  $-80$  °C. KRT23 expression was analyzed using a commercially available immunoassay according to the manufacturer's instructions (E5723m, Mouse ELISA Kit; E5723h, Human ELISA Kit; EIAab, Wuhan, China).

## Statistical Methods

SPSS 26.0 statistical software and GraphPad Prism 8.5 software were used for statistical analysis and plot the experimental data. The data are presented as the means  $\pm$  standard errors of the means (SEMs). A *t* test was used for comparisons between groups; the  $\chi$  chi-square test was used for comparisons of count data. Binary logistic regression was used to detect possible risk factors for MAFLD with significant differences ( $p < 0.05$ ). R software was used for eQTL linear regression analysis.

## Results

### Identification of Common DEGs

In GSE89632, 20818 variables exist, with the green dots indicating  $|\log_2FC| > 1$  and the blue dots indicating  $P < 0.0001$ . The red dots are DEGs that meet the above two requirements. Among the 490 DEGs, 209 genes were upregulated, and

281 genes were downregulated. In the heatmap from unsupervised hierarchical clustering analysis, healthy individuals presented substantially different gene expression profiles from those of MASH patients (Figure 2A and B).

## GO, KEGG Pathway Enrichment and PPI Network Establishment

To identify the functional categories of the DEGs, we analyzed the data through GO annotation between patients with and without MAFLD (Figure 2C). The enriched GO terms with  $P < 0.05$  included biological process (BP), cellular component (CC) and molecular function (MF).

In the BP category, the top five GO biological process terms were multicellular organism process, fat cell differentiation-neutrophil chemotaxis, gastrulation, oligodendrocyte differentiation, and mesenchyme development; in the CC category, the top six GO cellular component terms were apical part of cell, apical plasma membrane, membrane raft, chromocenter, membrane microdomain, and basolateral plasma membrane. In terms of MF frequency, the top six GO molecular function terms were signaling receptor activator activity, receptor ligand activity, cytokine activity chemokine activity, modified amino acid transmembrane transporter activity, dicarboxylic acid transmembrane transporter activity, and active transmembrane transporter activity.

KEGG pathway analysis revealed significant enrichment of terms related to cytokine–cytokine receptor interactions, viral protein interactions with cytokines and cytokine receptors, the TNF signaling pathway, the IL-17 signaling pathway, rheumatoid arthritis, primary immunodeficiency, the NF-kappa B signaling pathway, galactose metabolism, hypertrophic cardiomyopathy, and Chagas disease (Figure 2C and D).

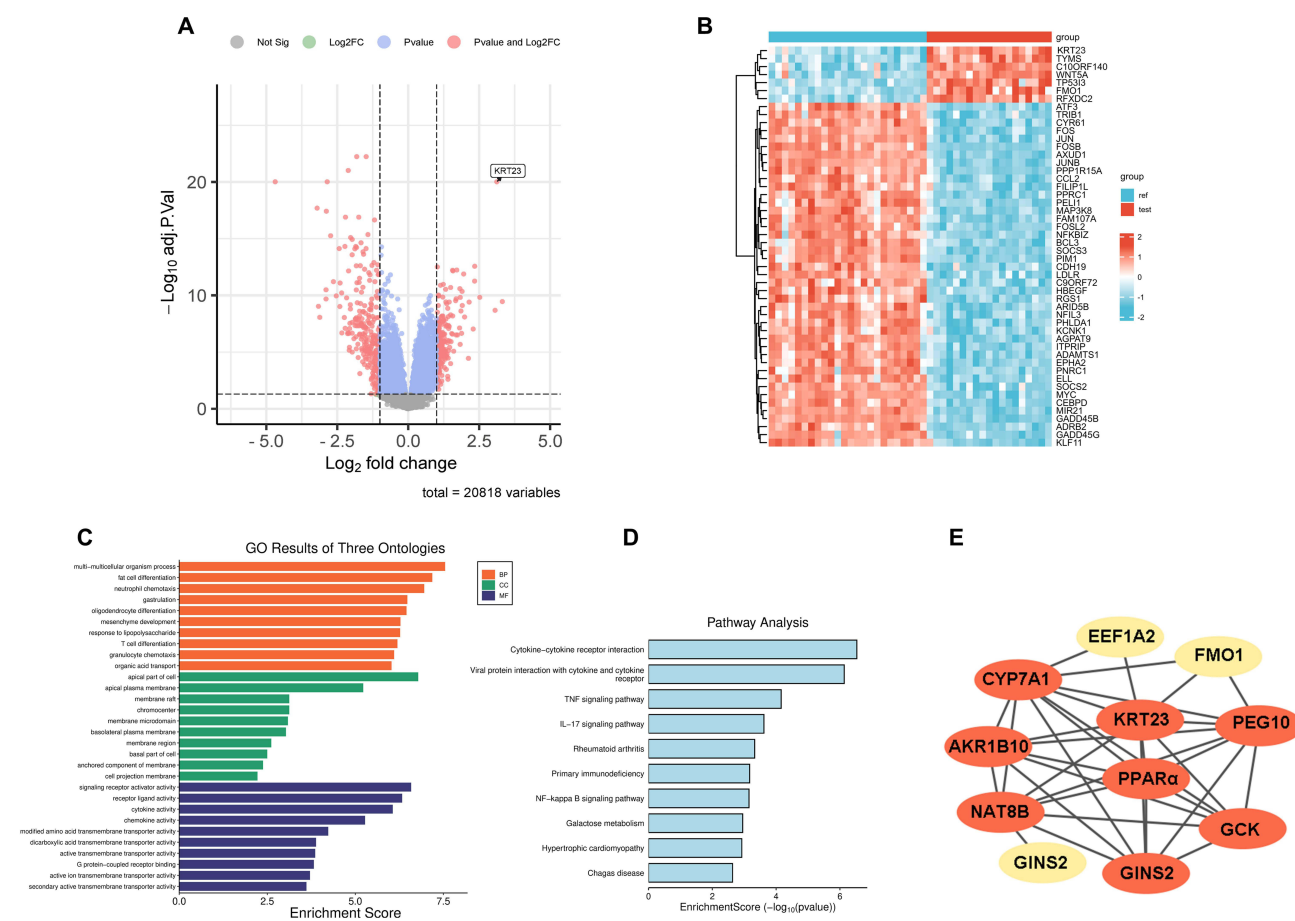


**Figure 2** Identification of differentially expressed genes (DEGs) in Metabolic dysfunction associated steatohepatitis (MASH) (GSE89632) using GEO2R. **(A)** Volcano plots of the DEGs in GSE89632. The negative  $\log_{10}$ -transformed adjusted P values (Y axis) are plotted against the average  $\log_2$ -fold changes (X axis) in gene expression. The identified DEGs are shown in red ( $\log_2\text{FC} > 1$ ) and blue ( $\log_2\text{FC} < -1$ ) with adjusted  $P < 0.05$ . **(B)** Heatmap of the DEGs in GSE89632. **(C)** To identify the functional categories of DEGs between patients with and without MAFLD through GO annotation. The enriched GO terms with  $P < 0.05$  included biological process (BP), cellular component (CC) and molecular function (MF). **(D)** KEGG pathway analysis. **(E)** Protein–protein interaction (PPI) network establishment and identification of hub genes.

To further investigate the molecular mechanism of the interactive relationships among all the DEGs, we mapped the DEGs to the STRING database and constructed a PPI network. In this PPI network, KRT23 could interact with metabolism-related proteins such as PPAR $\alpha$ , FMO1, CYP7A1 and GCK and tumor-related proteins such as EEF1A2, AKR1B10, GINS2 and PEG10 (Figure 2E).

## eQTL

The eQTL results showed significant association between the rs72826004 locus polymorphism of the KRT23 gene and its expression levels in serum ( $P < 0.001$ ). The KRT23 gene expression level in serum was significantly increased in MAFLD patients regardless of the genotype (GG genotype  $1.25 \pm 0.43$  vs  $3.31 \pm 0.82$  ng/mL,  $P < 0.001$ , GT genotype  $1.26 \pm 0.40$  vs  $3.07 \pm 0.59$  ng/mL,  $P < 0.001$ , TT genotype  $1.76 \pm 0.29$  vs  $4.40 \pm 2.02$  ng/mL,  $P < 0.001$ , Figure 3A).

That was showed no significant difference the association between with plasma KRT23 expression and rs2259859 locus polymorphism in eQTL analysis, but compare to MAFLD patients carrying rs2259859 locus CC and CT genotypes, those carrying the TT genotype showed lower KRT23 expression levels (CC genotype  $1.30 \pm 0.42$  vs  $3.57 \pm 1.36$ ,  $P < 0.001$ , CT genotype  $1.33 \pm 0.43$  vs  $2.45 \pm 1.26$ ,  $P < 0.001$ , TT genotype  $1.71 \pm 1.05$  vs  $2.32 \pm 0.01$ ,  $P < 0.001$ , Figure 3B).

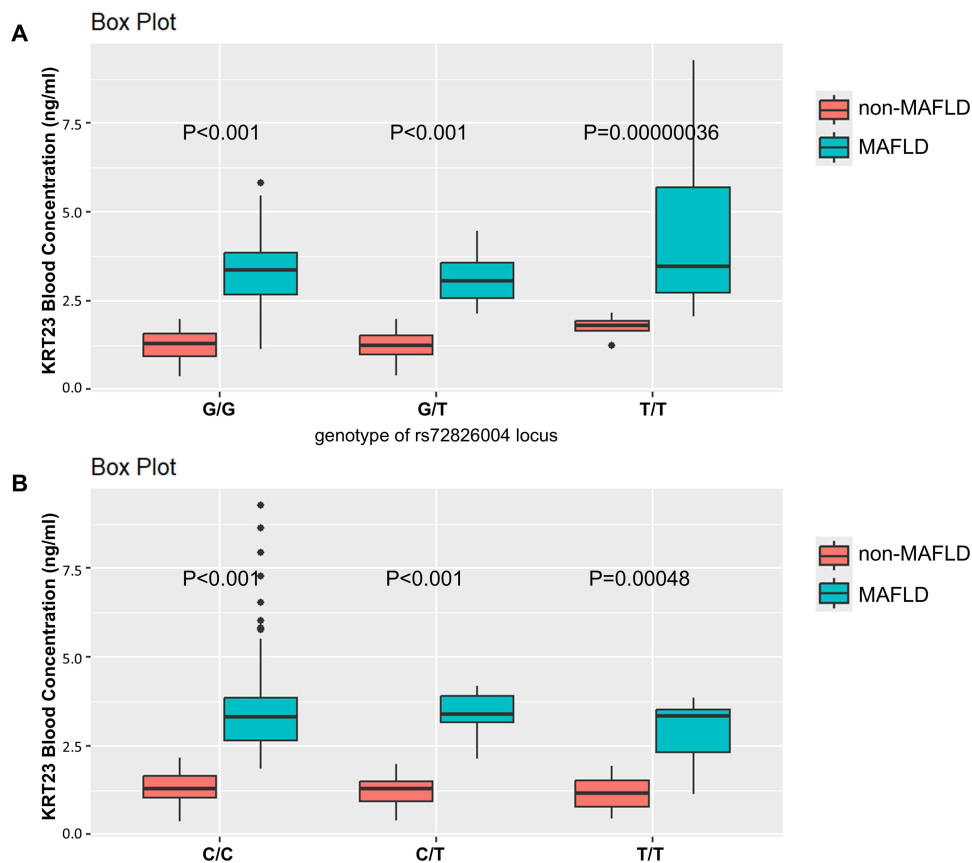


**Figure 3** Box plot of the KRT23 gene expression level in serum and KRT23 gene polymorphism in MAFLD patients. **(A)** The KRT23 gene expression level in serum was significantly increased in MAFLD patients with the rs72826004 locus elevated regardless of the genotype (GG genotype  $1.25 \pm 0.43$  vs  $3.31 \pm 0.82$ ,  $P < 0.001$ , GT genotype  $1.26 \pm 0.40$  vs  $3.07 \pm 0.59$ ,  $P < 0.001$ , TT genotype  $1.76 \pm 0.29$  vs  $4.40 \pm 2.02$ ,  $P < 0.001$ ). The eQTL analysis between rs72826004 locus polymorphism of KRT23 gene and serum expression showed statistically significant differences ( $P < 0.001$ , False Discovery Rate (FDR)  $< 0.001$ ). **(B)** Compare to MAFLD patients carrying rs2259859 locus CC and CT genotypes, those carrying the TT genotype showed lower KRT23 expression levels (CC genotype  $1.30 \pm 0.42$  vs  $3.57 \pm 1.36$ ,  $P < 0.001$ , CT genotype  $1.33 \pm 0.43$  vs  $2.45 \pm 1.26$ ,  $P < 0.001$ , TT genotype  $1.71 \pm 1.05$  vs  $2.32 \pm 0.01$ ,  $P < 0.001$ ).

## General Clinical Characteristics

In the KRT23 polymorphism study, MAFLD patients tended to be older ( $45.96 \pm 12.89$  vs  $52.35 \pm 13.61$  years,  $P < 0.001$ ) and were more likely to be male (289 (31.8%) vs 620 (68.2%),  $P < 0.001$ ). Compared with individuals without MAFLD, patients with MAFLD were more likely to smoke (180 (20.7%) vs 268 (29.9%),  $P < 0.001$ ), drink (319 (36.8%) vs 342 (38.3%),  $P < 0.001$ ), have hypertension (163 (18.2%) vs 525 (58.5%),  $P < 0.001$ ), have T2DM (73 (8.1%) vs 329 (36.6%),  $P < 0.001$ ), be obese (380 (43.0%) vs 783 (87.4%),  $P < 0.001$ ), and have CAD (37 (4.1%) vs 235 (26.3%),  $P < 0.001$ ). Compared with individuals without MAFLD, patients with MAFLD presented poor control of blood pressure (SBP  $119 \pm 16$  vs  $127 \pm 17$  mmHg,  $P < 0.001$ , DBP  $74 \pm 11$  vs  $79 \pm 11$  mmHg,  $P < 0.001$ ), HbA1c ( $5.66$  (5.38–6.1) vs  $5.70$  (5.39–6.41) %,  $P = 0.022$ ), glucose ( $5.38 \pm 1.82$  vs  $5.79 \pm 2.14$  mmol/L,  $P < 0.001$ ), ALT (20 (14.8–29.49) vs 22.01 (15.3–32.75) U/L,  $P = 0.003$ ) and LDL-c ( $2.75 \pm 0.69$  vs  $2.82 \pm 0.79$  mmol/L,  $P = 0.042$ , [Table 1](#)).

## KRT23 Gene rs72826004 and rs2269859 Loci Were Associated with MAFLD

KRT23 gene loci, including rs72826004 and rs2269859, were associated with MAFLD. The TT genotype of the KRT23 gene locus rs72826004 tended to increase the probability of MAFLD (32 (37.6%) vs 53 (62.4%),  $P = 0.027$ , [Table 2](#) and [Supplementary Figure 1A](#)), and the TT genotype of the KRT23 gene locus rs2269859 tended to protect individuals from MAFLD (37 (68.5%) vs 17 (31.5%),  $P = 0.004$ , [Table 2](#) and [Supplementary Figure 1B](#)).

**Table 1** General Characteristics of Patients with or without MAFLD

Characteristics	Non-MAFLD (n=886) (n=886)	MAFLD (n=909) (n=909)	P-value
Gender, n (%)			
Female	420 (47.4)	289 (31.8)	<0.001
Male	466 (52.6)	620 (68.2)	
Age, years	$45.96 \pm 12.89$	$52.35 \pm 13.61$	<0.001
Body Mass Index (BMI)	23.46 (21.4–25.47)	27.6 (25.0–30.0)	<0.001
Smoker, n (%)	180 (20.7)	268 (29.9)	<0.001
Drinking, n (%)	319 (36.8)	342 (38.3)	<0.001
Hypertension, n (%)	163 (18.2)	525 (58.5)	<0.001
CAD, n (%)	37 (4.1)	235 (26.3)	<0.001
T2DM, n (%)	73 (8.1)	329 (36.6)	<0.001
Dyslipidemia, n (%)	734 (81.8)	733 (81.6)	0.912
SBP (mmHg)	$119 \pm 16$	$127 \pm 17$	<0.001
DBP (mmHg)	$74 \pm 11$	$79 \pm 11$	<0.001
Obesity	380 (43.0)	783 (87.4)	<0.001
HGB (g/L)	$143.98 \pm 15.77$	$146.06 \pm 18.59$	0.011
Platelet ( $\times 10^9/L$ )	$245.22 \pm 55.9$	$250.21 \pm 65.29$	0.083
HbA1c (%)	5.66 (5.38–6.1)	5.70 (5.39–6.41)	0.022
FPG (mmol/L)	$5.38 \pm 1.82$	$5.79 \pm 2.14$	<0.001
ALB (U/L)	$44.11 \pm 2.5$	$44.38 \pm 2.42$	0.041
AST (U/L)	21.82 (18.3–27.38)	22.17 (18.33–27.54)	0.180
ALT (U/L)	20 (14.8–29.49)	22.01 (15.3–32.75)	0.003
ALP (U/L)	68.56 (55.3–82.84)	58.5 (56.6–83.36)	0.481
Creatinine (umol/L)	67.12 (55.67–78.66)	68.22 (57.62–79.38)	0.121
TG (mmol/L)	1.33 (0.94–1.97)	1.38 (0.95–2.2)	0.120
TC (mmol/L)	$4.38 \pm 0.99$	$4.42 \pm 0.99$	0.365
HDL-C (mmol/L)	$1.15 \pm 0.30$	$1.15 \pm 0.44$	0.700
LDL-C (mmol/L)	$2.75 \pm 0.69$	$2.82 \pm 0.79$	0.042

**Note:**  $P < 0.05$  was considered significant difference.

**Abbreviations:** MAFLD, Metabolic Dysfunction-Associated Fatty Liver Disease; T2DM, Type 2 Diabetes Mellitus; CAD, Coronary Artery Disease; SBP, Systolic Blood Pressure; DBP, Diastolic Blood Pressure; BMI, Body Mass Index; Obesity:  $BMI \geq 28$ ; HGB, Hemoglobin; HbA1c, Hemoglobin A1C; FPG, Fasting plasma Glucose; TG, Triglyceride; TC, Total Cholesterol; LDL-C, Low-Density Lipoprotein Cholesterol; HDL-C, High-Density Lipoprotein Cholesterol; ALT, Alanine Transferase; AST, Aspartate Transferase; HbA1c, Hemoglobin A1C.

**Table 2** KRT23 Gene Polymorphisms in Patients with or without MAFLD

Polymorphisms	Control (n=886)	MAFLD (n=909)	P-value
<b>rs7282004</b>			
GG+GT	854 (49.9)	856 (50.1)	0.027
TT	32 (37.6)	53 (62.4)	
<b>rs2269859</b>			
CC+CT	849 (48.8)	892 (51.2)	0.004
TT	37 (68.5)	17 (31.5)	

**Note:** P< 0.05 was considered significant difference.

**Abbreviation:** MAFLD, Metabolic Dysfunction-Associated Fatty Liver Disease.

## Risk Factors for MAFLD

As shown in [Figure 4](#) and [Supplementary Table 7](#), age, smoking, drinking, sex, TG, TC, HDL-C, LDL-C, glucose>6.1 mmol/L, hypertension, T2DM, CAD, obesity, the rs72826004 TT genotype and the rs2269859 TT genotype of KRT23 were included to construct a multivariate logistic risk model. Through univariate and multivariate logistic analysis, we found that smoking (OR: 1.589, 95% CI: 1.194–2.115, P=0.002), glucose>6.1 mmol/L (OR: 1.745, 95% CI: 1.242–2.451, P=0.001), hypertension (OR: 3.77, 95% CI: 2.884–4.927, P<0.001), T2DM (OR: 1.952, 95% CI: 1.433–2.659, P<0.001), CAD (OR: 6.724, 95% CI: 4.181–10.813, P<0.001), obesity (OR: 7.476, 95% CI: 5.613–9.958, P<0.001), and the rs72826004 TT (OR: 2.082, 95% CI: 1.153–3.757, P=0.015) genotype may be risk factors for MAFLD, while the rs2269859 TT (OR: 0.317, 95% CI: 0.154–0.651, P=0.002) genotype may be a protective factor for MAFLD.

Compared with patients MAFLD without CAD patients, smoking (OR: 2.021, 95% CI 1.283–3.183; P=0.002), hypertension (OR: 2.118, 95% CI 1.485–3.022; P<0.001), glucose > 6.1 mmol/L (OR: 1.095, 95% CI 1.075–1.115; P<0.001), T2DM (OR: 1.425, 95% CI 1.002–2.027; P=0.049), and rs2269859 (OR: 5.442, 95% CI 1.908–15.522, P=0.002) may be risk factors of the MAFLD combined with CAD. HDL-c (OR: 0.371, 95% CI 0.182–0.754; P=0.006), drinking (OR: 0.187, 95% CI 0.116–0.302; P<0.001) may be protective factors of the MAFLD combined with CAD ([Supplementary Figure 2A](#)).

Compared with MAFLD without T2DM, rs72826004 (OR: 2.392, 95% CI 1.31–4.366, P=0.005), glucose > 6.1 mmol/L (OR: 1.802, 95% CI 1.039–3.126, P=0.036) may be risk factors of the MAFLD combined with T2DM ([Supplementary Figure 2B](#)).

## Increased KRT23 Expression Is Related to MAFLD in Humans and Mice

Compared with individuals without MAFLDs, patients with MAFLD presented greater lipid deposition ( $1.00 \pm 0.1$  vs  $1.66 \pm 0.21$ , P=0.0083, Oil Red O staining, [Figure 5A](#), iii, iv and C); MAFLD patients presented greater KRT23

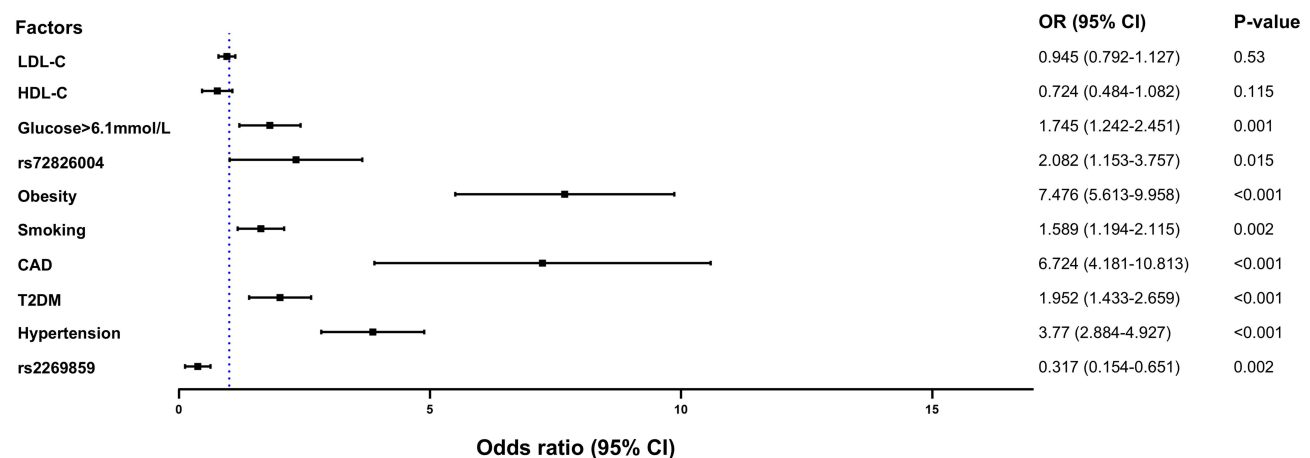


**Figure 4** Logistic regression analysis of risk factors for MAFLD.

**Abbreviations:** OR, odds ratio; CI, confidence interval; Obesity; BMI, Body Mass Index > 28; CAD, Coronary Artery Disease; T2DM, Type 2 Diabetes Mellitus.

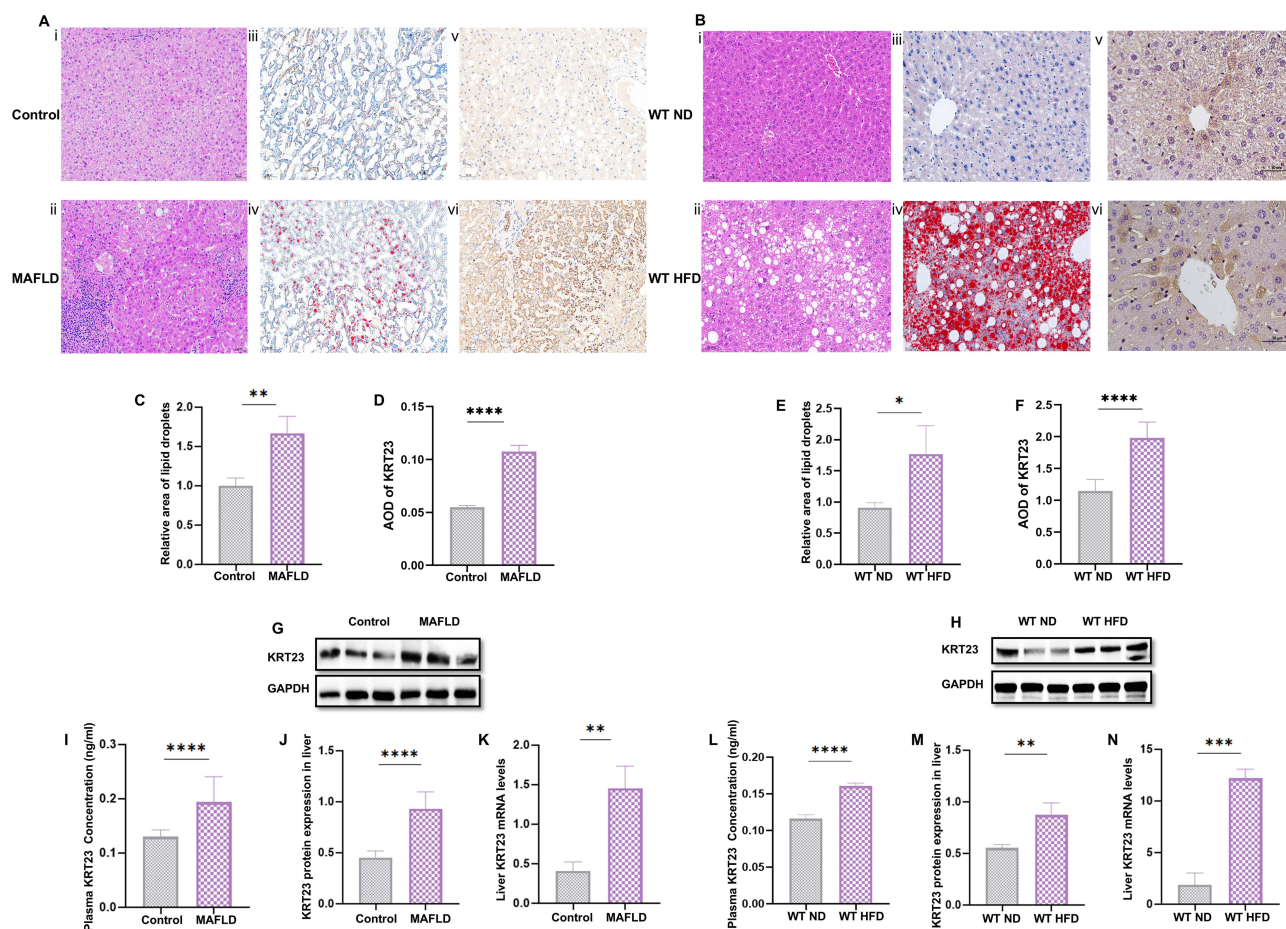


**Figure 5** Elevated expression of the KRT23 gene in individuals and mice with MAFLD. **(A)** Histological changes in liver of MAFLD patients. i: HE staining of the livers of non-MAFLD; ii: HE staining of the livers of MAFLD patients showed fat like or balloon like changes in liver cells; iii: Oil red O staining of the livers of non-MAFLD; iv: Oil red O staining of the livers of MAFLD patients shows more deposition of lipid droplets; v: KRT23 immunohistochemistry (IHC) of non-MAFLD (control); vi: KRT23 IHC of MAFLD patients. **(B)** Histological changes in MAFLD mice model. i: HE staining of the livers of WT ND (control); ii: HE staining of the livers of MAFLD mice showed that the MAFLD mice exhibited fat like or balloon like changes in liver cells; iii: Oil red O staining shows the deposition of lipid droplets; iv: analysis of relative area of lipid droplets in liver tissue of MAFLD patients; v: KRT23 IHC of WT ND (control); vi: KRT23 IHC of MAFLD mice. **(C)** Compared with non-MAFLD individuals, MAFLD patients presented greater lipid deposition ( $1.00 \pm 0.1$  vs  $1.66 \pm 0.21$ ,  $P=0.0083$ ). **(D)** For average optical density (AOD) in KRT23 IHC test, MAFLD patient was higher than non-MAFLD individuals ( $0.06 \pm 0.002$  vs  $0.11 \pm 0.009$ ,  $P=0.0005$ ). **(E)** MAFLD mice presented greater lipid deposition ( $1.23 \pm 0.27$  vs  $1.91 \pm 0.35$ ,  $P=0.0026$ ). **(F)** Compared with non-MAFLD mice, AOD of KRT23 IHC test, MAFLD mice presented greater lipid deposition ( $1.23 \pm 0.27$  vs  $1.91 \pm 0.35$ ,  $P=0.0026$ ). Western blotting analysis showed higher expression of KRT23 in liver of MAFLD patients **(G and J)** and animal model **(H and M)** compared with controls. Plasma KRT23 concentration increased in MAFLD patients **(I)** and MAFLD mice models **(L)** compared with controls. MAFLD patients **(K)** and MAFLD mice models **(N)** showed higher liver KRT23 mRNA compared with controls. **Notes:** \* $P < 0.05$ , \*\* $P < 0.01$ , \*\*\* $P < 0.001$ , and \*\*\*\* $P < 0.0001$ .

expression in serum ( $0.12 \pm 0.01$  vs  $0.19 \pm 0.05$ ,  $P < 0.0001$ , [Figure 5I](#)) and liver tissue ( $0.45 \pm 0.06$  vs  $0.93 \pm 0.06$ ,  $P < 0.0001$ , [Figure 5G and J](#)). This finding was confirmed through an IHC test ( $0.06 \pm 0.001$  vs  $0.11 \pm 0.006$ ,  $P < 0.0001$ , [Figure 5A, v, vi and D](#)). KRT23 mRNA expression was increased in patients with MAFLD patients (qRT-PCR:  $1.87 \pm 1.15$  vs  $12.18 \pm 0.89$ ,  $P < 0.0001$ , [Figure 5K](#)).

Compared with mice fed a normal diet, those fed a HFD (MAFLD) presented greater lipid deposition (Oil Red O staining,  $0.91 \pm 0.08$  vs  $1.77 \pm 0.46$ ,  $P=0.0327$ ; [Figure 5B, iii, iv and E](#)). MAFLD mice expressed more KRT23 protein, including serum ( $0.12 \pm 0.005$  vs  $0.16 \pm 0.004$ ,  $P < 0.001$ , [Figure 5L](#)), liver tissue ( $0.55 \pm 0.03$  vs  $0.87 \pm 0.12$ ,  $P=0.0012$ , [Figure 5H and M](#)), and qRT-PCR ( $1.87 \pm 1.15$  vs  $12.18 \pm 0.89$ ,  $P < 0.0001$ , [Figure 5N](#)). This finding was confirmed through IHC ( $1.15 \pm 0.18$  vs  $1.98 \pm 0.25$ ,  $P < 0.0001$ , [Figure 5B, v, vi and F](#)). and in db/db model liver tissue ( $0.44 \pm 0.09$  vs  $1.18 \pm 0.14$ ,  $P < 0.0001$ , [Supplementary Figure 3A](#) (HE staining of liver in WT mice), [Supplementary Figure 3B](#) (HE staining of liver in db/db mice), [Supplementary Figure 3C](#) (Representative Western blot bands of KRT23 and GAPDH in liver tissues of WT and db/db mice), [Supplementary Figure 3D](#) (Quantitative analysis of KRT23 protein

levels, standardized to GAPDH), qRT-PCR ( $0.63 \pm 0.11$  vs  $1.73 \pm 0.28$ ,  $P < 0.001$ , [Supplementary Figure 3E](#)). We scored 6 patients with MASH and 5 patients without MASH ( $0.8 \pm 0.84$  vs  $5.5 \pm 1.05$ ,  $P < 0.0001$ ).

## Discussion

In this study, enrichment analyses revealed that ten DEGs were involved in MAFLD and that KRT23 played important roles in the pathogenesis of MAFLD. KRT23 gene polymorphism was found to be related to the incidence of MAFLD compared with non-MAFLD individuals. The TT genotype of KRT23 rs72826004 tended to increase the incidence of MAFLD, whereas the TT genotype of rs2269859 may have potential roles in protection from MAFLD. KRT23 expression was increased in the serum and liver of MAFLD patients. In the MAFLD mouse model, increased KRT23 expression was confirmed.

Previous studies have shown that KRT affects various cellular processes, including cell signaling, apoptosis, and the stress response, thereby expanding the classical role of KRT in the formation of cytoskeleton components such as intermediate filaments.<sup>32–34</sup> Krt7, Krt8, Krt10, Krt18, Krt19, and Krt20 are commonly used as prognostic and diagnostic markers for liver disease and cancer.<sup>35</sup> KRT7, KRT19, and KRT23 are considered as biomarkers of ductular reaction (DR).<sup>12,33,36</sup> Odena et al identified KRT23 as a novel marker for ductal cells.<sup>17</sup> The potential pathology of DR leads to extensive tissue remodeling in chronic liver disease. DR is a characteristic response to liver injury that is closely related to progressive fibrosis and inflammation in many chronic liver diseases.<sup>12</sup>

We found that KRT23 was related to MASH in the database. MASH is a severe type of MAFLD, and they have similar mechanism including insulin resistance, oxidative stress, and inflammatory signaling.<sup>37,38</sup> On this basis, we speculated that KRT23 may also affect the development of MAFLD, so KRT23 was chosen as our candidate gene for further analysis.

As a key regulatory factor for liver lipid metabolism and energy balance, the role of PPAR  $\alpha$  in MAFLD is dual, as it exerts protective effects by improving lipid metabolism and may also promote disease progression or cancer risk under specific conditions. In the early stage of NAFLD (simple steatosis) or acute stress (such as fasting, short-term high-fat diet), the liver promotes fatty acid oxidation through the activation of PPAR  $\alpha$ , which is an adaptive protective response.<sup>18,39</sup> As the disease progresses to NASH or fibrosis stage, chronic inflammation, oxidative stress, and lipotoxicity can inhibit PPAR  $\alpha$  expression, leading to a decrease in its transcriptional activity.<sup>40,41</sup> Francque, Sven et al found that PPAR  $\alpha$  levels were lower in the liver of NASH patients.<sup>42</sup> Kim D. et al confirms that PPAR  $\alpha$  activation (such as drug or metabolic stress) significantly upregulates KRT23 expression (>40 fold) and relies on the synergistic effect of MYC.<sup>43</sup> Future research needs to further differentiate the dynamic changes and clinical significance of PPAR  $\alpha$  expression and activity. R Díaz-Rúa et al reported that liver KTR23 levels (mRNA and protein) were elevated in mice fed high-calorie and high-fat diets.<sup>44</sup> And this is consistent with our findings.

Both genetic and environmental factors can influence the pathogenesis of disease.<sup>45</sup> For example, the KRT23 rs72826004 locus TC + CC genotype plays important roles in aggressive periodontitis and severe chronic periodontitis in Japanese people.<sup>46</sup> And genetic factors are believed to play a primary role in MAFLD occurrence.<sup>47</sup> Gene polymorphism may influence the expression of target protein.<sup>48</sup> As eQTL results showed biologically meaningful association between the rs72826004 locus of the KRT23 gene and its expression levels in serum. The rs72826004 locus of the KRT23 gene is located in the 5'-flanking region and is involved in regulating the expression of genetic information. The rs2269859 locus of the KRT23 gene is in exon 2. The 5'-spreading region is located at the 5' end of a gene, adjacent to the starting point, and typically includes transcription regulatory sequences (TRS) and transcription factor-binding sites (TFBS), family regulatory pathways, and enhancers, thus affecting gene expression. Mutations in exons can lead to changes in the composition or arrangement of bases in the coding region, resulting in altered gene structure and expression.<sup>49</sup> Both of these factors may affect disease susceptibility.

MAFLD is considered as a risk factor for CAD, as we confirmed in this study.<sup>50</sup> MAFLD is also an independent risk factor for T2DM.<sup>51</sup> Interestingly, KRT23 polymorphism contributes not only to MAFLD but also to MAFLD combined with T2DM and CAD. Several mechanisms are involved in MAFLD combined with CVD, such as hepatic insulin resistance, systemic low-grade inflammation, adhesion molecules, and a pro-thrombotic state.<sup>52</sup> MAFLD is associated with hepatic and peripheral insulin resistance, resulting in insufficient suppression of hepatic gluconeogenesis, decreased glycogen synthesis and increased lipid accumulation.<sup>53</sup>

The present study is the first to examine the associations between MAFLD and KRT23 SNPs. Although higher expression was confirmed in MAFLD patients and animal MAFLD models. However, the detailed mechanism of the association between KRT23 and MAFLD is unclear. More detailed SNP analysis and functional analysis of these SNPs are needed. Understanding the roles of genetic and clinical factors could be valuable for more targeted interventions selection, improving the prognosis of patients with MAFLD. Further experimental research is needed to explore the specific roles and regulatory mechanisms of KRT23 and related genes in the pathogenesis of MAFLD.

## Limitations

This study also has several limitations. First, the participants in this study were recruited only at the First Affiliated Hospital of Xinjiang Medical University, which may not necessarily reflect the true occurrence of MAFLD at the provincial or national level, as well as the true occurrence of MAFLD combined with CAD and T2DM. Second, owing to the large sample size, liver biopsy was not performed on all individuals to diagnose MAFLD.

## Conclusion

In conclusion, in the present study, (1) bioinformatics analysis revealed potential roles for KRT23 in MAFLD. (2) KRT23 gene polymorphism was associated with the occurrence of MAFLD. (3) Individuals carrying the KRT23 rs72826004 locus (TT genotype) tended to have more MAFLD. Individuals carrying the KRT23 rs2269859 locus (TT genotype) tended to be opposed to MAFLD. (4) KRT23 expression was positively associated with MAFLD, which was confirmed in both human and animal MAFLD models. KRT23 is a clinically actionable target for MAFLD.

## Highlight

- Bioinformatics analysis revealed potential roles for KRT23 in MAFLD.
- KRT23 gene polymorphism was associated with the occurrence of MAFLD.
- KRT23 expression was positively associated with MAFLD, which was confirmed in both human and animal MAFLD models.
- KRT23 is a potential therapeutical target for MAFLD.

## Ethic Declaration

This study was approved by the Ethics Committee of the First Affiliated Hospital of Xinjiang Medical University (Urumqi, China) and conducted according to the standards of the Declaration of Helsinki and written informed consents were obtained from all the participants.

## Author Contributions

All authors made a significant contribution to the work reported, whether that is in the conception, study design, execution, acquisition of data, analysis and interpretation, or in all these areas; took part in drafting, revising or critically reviewing the article; gave final approval of the version to be published; have agreed on the journal to which the article has been submitted; and agree to be accountable for all aspects of the work.

## Funding

The survey was funded by the Xinjiang Young Scientific and Technical Talents Training Project (2019Q040), Natural Science Foundation of Xinjiang Uygur Autonomous Region, Outstanding Youth Science Foundation Project (2021D01E28), the National Natural Science Foundation of China (81960078), State Key Laboratory of Pathogenesis, Prevention and Treatment of High Incidence Diseases in Central Asia, Xinjiang Medical University (SKL-HIDCA-2021-XXG4, SKL-HIDCA-2024-1 and SKL-HIDCA-2024-BZ5), Xinjiang Youth Science and Technology Top Talents Special Project (2022TSYCCX0103) and Xinjiang Science and Technology Innovation Team (Tianshan Innovation Team, 2022TSYCT-D0014), Xinjiang Bayingolin Mongolian Autonomous Prefecture “Open bidding for selecting the best candidates” Project (202427).

## Disclosure

The authors declare no competing interests in this work.

## References

1. EASL. EASL-EASD-EASO Clinical Practice Guidelines for the management of non-alcoholic fatty liver disease. *J Hepatol.* 2016;64(6):1388–1402. doi:10.1016/j.jhep.2015.11.004
2. Chalasani N, Younossi Z, Lavine JE, et al. The diagnosis and management of nonalcoholic fatty liver disease: practice guidance from the American Association for the Study of Liver Diseases. *Hepatology.* 2018;67(1):328–357. doi:10.1002/hep.29367
3. Wong VW, Chan WK, Chitturi S, et al. Asia-Pacific Working Party on Non-alcoholic Fatty Liver Disease guidelines 2017-Part 1: definition, risk factors and assessment. *J Gastroenterol Hepatol.* 2018;33(1):70–85. doi:10.1111/jgh.13857
4. Lallukka S, Yki-Järvinen H. Non-alcoholic fatty liver disease and risk of type 2 diabetes. *Best Pract Res Clin Endocrinol Metab.* 2016;30(3):385–395. doi:10.1016/j.beem.2016.06.006
5. Sung KC, Jeong WS, Wild SH, Byrne CD. Combined influence of insulin resistance, overweight/obesity, and fatty liver as risk factors for type 2 diabetes. *Diabetes Care.* 2012;35(4):717–722. doi:10.2337/dc11-1853
6. Medina-Santillán R, López-Velázquez JA, Chávez-Tapia N, Torres-Villalobos G, Uribe M, Méndez-Sánchez N. Hepatic manifestations of metabolic syndrome. *Diabetes Metab Res Rev.* 2013. doi:10.1002/dmrr.2410
7. Ye Q, Zou B, Yeo YH, et al. Global prevalence, incidence, and outcomes of non-obese or lean non-alcoholic fatty liver disease: a systematic review and meta-analysis. *Lancet Gastroenterol Hepatol.* 2020;5(8):739–752. doi:10.1016/s2468-1253(20)30077-7
8. Younossi ZM, Koenig AB, Abdelatif D, Fazel Y, Henry L, Wymer M. Global epidemiology of nonalcoholic fatty liver disease-Meta-analytic assessment of prevalence, incidence, and outcomes. *Hepatology.* 2016;64(1):73–84. doi:10.1002/hep.28431
9. Hagström H, Shang Y, Hegmar H, Nasr P. Natural history and progression of metabolic dysfunction-associated steatotic liver disease. *Lancet Gastroenterol Hepatol.* 2024;9(10):944–956. doi:10.1016/S2468-1253(24)00193-6
10. Rao G, Peng X, Li X, et al. Unmasking the enigma of lipid metabolism in metabolic dysfunction-associated steatotic liver disease: from mechanism to the clinic. Review. *Front Med.* 2023;10:1.
11. Wazir H, Abid M, Essani B, et al. Diagnosis and Treatment of Liver Disease: current Trends and Future Directions. *Cureus.* 2023;15(12):e49920. doi:10.7759/cureus.49920
12. Guldiken N, Kobazi Ensari G, Lahiri P, et al. Keratin 23 is a stress-inducible marker of mouse and human ductular reaction in liver disease. *J Hepatol.* 2016;65(3):552–559. doi:10.1016/j.jhep.2016.04.024
13. Redmond CJ, Coulombe PA. Intermediate filaments as effectors of differentiation. *Curr Opin Cell Biol.* 2021;68:155–162. doi:10.1016/j.ceb.2020.10.009
14. Liffers ST, Maghnoji A, Munding JB, et al. Keratin 23, a novel DPC4/Smad4 target gene which binds 14-3-3 $\epsilon$ . *BMC Cancer.* 2011;11(1):137. doi:10.1186/1471-2407-11-137
15. Birkenkamp-Demtroder K, Mansilla F, Sørensen FB, et al. Phosphoprotein Keratin 23 accumulates in MSS but not MSI colon cancers in vivo and impacts viability and proliferation in vitro. *Mol Oncol.* 2007;1(2):181–195.
16. Starmann J, Fälth M, Spindelböck W, et al. Gene expression profiling unravels cancer-related hepatic molecular signatures in steatohepatitis but not in steatosis. *PLoS One.* 2012;7(10):e46584. doi:10.1371/journal.pone.0046584
17. Odena G, Chen J, Lozano JJ, et al. LPS-TLR4 Pathway Mediates Ductular Cell Expansion in Alcoholic Hepatitis. *Sci Rep.* 2016;6(1):35610. doi:10.1038/srep35610
18. Régnier M, Polizzi A, Lippi Y, et al. Insights into the role of hepatocyte PPAR $\alpha$  activity in response to fasting. *Mol Cellular Endocrinol.* 2018;471:75–88. doi:10.1016/j.mce.2017.07.035
19. Barrett T, Wilhite SE, Ledoux P, et al. NCBI GEO: archive for functional genomics data sets--update. *Nucleic Acids Res.* 2013;41(Database issue):D991–5. doi:10.1093/nar/gks1193
20. EAftSot L. Diabetes EAftSo, Obesity EAftSo. EASL-EASD-EASO Clinical Practice Guidelines on the management of metabolic dysfunction-associated steatotic liver disease (MASLD). *Obesity Facts.* 2024;17(4):374–443.
21. Liu C, Pan Y, Li Q, Zhang Y. Bioinformatics analysis identified differentially expressed genes as potential biomarkers for Hashimoto's thyroiditis-related papillary thyroid cancer. *Int J Med Sci.* 2021;18(15):3478–3487. doi:10.7150/ijms.63402
22. Tannapfel A, Denk H, Dienes HP, et al. Histopathological diagnosis of non-alcoholic and alcoholic fatty liver disease. *Virchows Arch.* 2011;458(5):511–523. doi:10.1007/s00428-011-1066-1
23. Hsu CL, Loomba R. From NAFLD to MASLD: implications of the new nomenclature for preclinical and clinical research. *Nat Metab.* 2024;6(4):600–602. doi:10.1038/s42255-024-00985-1
24. Arai T, Atsukawa M, Tsubota A, et al. Antifibrotic effect and long-term outcome of SGLT2 inhibitors in patients with NAFLD complicated by diabetes mellitus. *Hepatol Commun.* 2022;6(11):3073–3082. doi:10.1002/hep4.2069
25. Eslam M, Newsome PN, Sarin SK, et al. A new definition for metabolic dysfunction-associated fatty liver disease: an international expert consensus statement. *J Hepatol.* 2020;73(1):202–209. doi:10.1016/j.jhep.2020.03.039
26. Kim JW, Lee Y-S, Park YS, et al. Multiparametric MR Index for the Diagnosis of Non-Alcoholic Steatohepatitis in Patients with Non-Alcoholic Fatty Liver Disease. *Sci Rep.* 2020;10(1):2671. doi:10.1038/s41598-020-59601-3
27. American Diabetes Association. Classification and Diagnosis of Diabetes: standards of Medical Care in Diabetes-2019. *Diabetes Care.* 2019;42(Suppl 1):S13–s28. doi:10.2337/dc19-S002
28. Levine GN, Bates ER, Bittl JA, et al. ACC/AHA Guideline Focused Update on Duration of Dual Antiplatelet Therapy in Patients With Coronary Artery Disease: a Report of the American College of Cardiology/American Heart Association Task Force on Clinical Practice Guidelines: an Update of the 2011 ACCF/AHA/SCAI Guideline for Percutaneous Coronary Intervention, 2011 ACCF/AHA Guideline for Coronary Artery Bypass Graft Surgery, 2012 ACC/AHA/ACP/AATS/PCNA/SCAI/STS Guideline for the Diagnosis and Management of Patients With Stable Ischemic Heart Disease, 2013 ACCF/AHA Guideline for the Management of ST-Elevation Myocardial Infarction, 2014 AHA/ACC Guideline for the

- Management of Patients With Non-ST-Elevation Acute Coronary Syndromes, and 2014 ACC/AHA Guideline on Perioperative Cardiovascular Evaluation and Management of Patients Undergoing Noncardiac Surgery. *Circulation*. 2016;134(10):e123–55. doi:10.1161/cir.0000000000000404
29. Samad H, Coll F, Preston MD, Ocholla H, Fairhurst RM, Clark TG. Imputation-based population genetics analysis of *Plasmodium falciparum* malaria parasites. *PLoS Genetics*. 2015;11(4):e1005131. doi:10.1371/journal.pgen.1005131
  30. Liang W, Menke AL, Driessen A, et al. Establishment of a general NAFLD scoring system for rodent models and comparison to human liver pathology. *PLoS One*. 2014;9(12):e115922. doi:10.1371/journal.pone.0115922
  31. Zhao F, Maren NA, Kosentka PZ, et al. An optimized protocol for stepwise optimization of real-time RT-PCR analysis. *Hortic Res*. 2021;8(1). doi:10.1038/s41438-021-00616-w.
  32. Gu LH, Coulombe PA. Keratin function in skin epithelia: a broadening palette with surprising shades. *Curr Opin Cell Biol*. 2007;19(1):13–23. doi:10.1016/j.ceb.2006.12.007
  33. Omary MB, Ku NO, Strnad P, Hanada S. Toward unraveling the complexity of simple epithelial keratins in human disease. *J Clin Invest*. 2009;119(7):1794–1805. doi:10.1172/jci37762
  34. Haines RL, Lane EB. Keratins and disease at a glance. *J Cell Sci*. 2012;125(Pt 17):3923–3928. doi:10.1242/jcs.099655
  35. Takan I, Karakülah G, Louka A, Pavlopoulou A. “In the light of evolution”: keratins as exceptional tumor biomarkers. *PeerJ*. 2023;11:e15099. doi:10.7717/peerj.15099
  36. Strnad P, Paschke S, Jang KH, Ku NO. Keratins: markers and modulators of liver disease. *Curr Opin Gastroenterol*. 2012;28(3):209–216. doi:10.1097/MOG.0b013e3283525cb8
  37. Gancheva S, Roden M, Castera L. Diabetes as a risk factor for MASH progression. *Diabetes Res Clin Pract*. 2024;217:111846. doi:10.1016/j.diabres.2024.111846
  38. Gofton C, Upendran Y, Zheng M-H, George J. MAFLD: how is it different from NAFLD? *Clin Mol Hepatol*. 2022;29(Suppl):S17. doi:10.3350/cmh.2022.0367
  39. Donnelly KL, Smith CI, Schwarzenberg SJ, Jessurun J, Boldt MD, Parks EJ. Sources of fatty acids stored in liver and secreted via lipoproteins in patients with nonalcoholic fatty liver disease. *J Clin Invest*. 2005;115(5):1343–1351. doi:10.1172/JCI23621
  40. Todisco S, Santarsiero A, Convertini P, et al. PPAR alpha as a metabolic modulator of the liver: role in the pathogenesis of nonalcoholic steatohepatitis (NASH). *Biology*. 2022;11(5):792. doi:10.3390/biology11050792
  41. Cai D, Yuan M, Frantz DF, et al. Local and systemic insulin resistance resulting from hepatic activation of IKK- $\beta$  and NF- $\kappa$ B. *Nature Med*. 2005;11(2):183–190. doi:10.1038/nm1166
  42. Francque S, Verrijken A, Caron S, et al. PPAR $\alpha$  gene expression correlates with severity and histological treatment response in patients with non-alcoholic steatohepatitis. *J Hepatol*. 2015;63(1):164–173. doi:10.1016/j.jhep.2015.02.019
  43. Kim D, Brocker CN, Takahashi S, et al. Keratin 23 Is a Peroxisome Proliferator-Activated Receptor Alpha-Dependent, MYC-Amplified Oncogene That Promotes Hepatocyte Proliferation. *Hepatology*. 2019;70(1):154–167. doi:10.1002/hep.30530
  44. Díaz-Rúa R, van Schothorst EM, Keijer J, Palou A, Oliver P. Isocaloric high-fat feeding directs hepatic metabolism to handling of nutrient imbalance promoting liver fat deposition. *Int J Obesity*. 2016;40(8):1250–1259. doi:10.1038/ijo.2016.47
  45. Buzzetti E, Pinzani M, Tsochatzis EA. The multiple-hit pathogenesis of non-alcoholic fatty liver disease (NAFLD). *Metabolism*. 2016;65(8):1038–1048. doi:10.1016/j.metabol.2015.12.012
  46. Suzuki A, Ji G, Numabe Y, et al. Single nucleotide polymorphisms associated with aggressive periodontitis and severe chronic periodontitis in Japanese. *Biochem Biophys Res Commun*. 2004;317(3):887–892. doi:10.1016/j.bbrc.2004.03.126
  47. Sharma D, Mandal P. NAFLD: genetics and its clinical implications. *Clin Res Hepatol Gastroenterol*. 2022;46(9):102003. doi:10.1016/j.clinre.2022.102003
  48. El-Tahan RR, Ghoneim AM, El-Mashad N. TNF- $\alpha$  gene polymorphisms and expression. *Springerplus*. 2016;5(1):1–7. doi:10.1186/s40064-016-3197-y
  49. Zoghbi HY, Beaudet AL. Epigenetics and human disease. *Cold Spring Harbor Perspect Biol*. 2016;8(2):a019497. doi:10.1101/cshperspect.a019497
  50. Caussy C, Aubin A, Loomba R. The relationship between type 2 diabetes, NAFLD, and cardiovascular risk. *Curr Diabet Rep*. 2021;21(5):1–13. doi:10.1007/s11892-021-01383-7
  51. Yamazaki H, Tsuboya T, Tsuji K, Dohke M, Maguchi H. Independent Association Between Improvement of Nonalcoholic Fatty Liver Disease and Reduced Incidence of Type 2 Diabetes. *Diabetes Care*. 2015;38(9):1673–1679. doi:10.2337/dc15-0140
  52. Ballestri S, Lonardo A, Bonapace S, Byrne CD, Loria P, Targher G. Risk of cardiovascular, cardiac and arrhythmic complications in patients with non-alcoholic fatty liver disease. *World J Gastroenterol*. 2014;20(7):1724. doi:10.3748/wjg.v20.i7.1724
  53. Tilg H, Moschen AR, Roden M. NAFLD and diabetes mellitus. *Nat Rev Gastroenterol Hepatol*. 2017;14(1):32–42. doi:10.1038/nrgastro.2016.147

International Journal of General Medicine

Publish your work in this journal

The International Journal of General Medicine is an international, peer-reviewed open-access journal that focuses on general and internal medicine, pathogenesis, epidemiology, diagnosis, monitoring and treatment protocols. The journal is characterized by the rapid reporting of reviews, original research and clinical studies across all disease areas. The manuscript management system is completely online and includes a very quick and fair peer-review system, which is all easy to use. Visit <http://www.dovepress.com/testimonials.php> to read real quotes from published authors.

Submit your manuscript here: <https://www.dovepress.com/international-journal-of-general-medicine-journal>

**Dovepress**  
Taylor & Francis Group